Full paper

Applied Organometallic Chemistry

Received: 1 July 2015 Accepted: 21 July 2015 Published online in Wiley Online Library: 11 September 2015

(wileyonlinelibrary.com) DOI 10.1002/aoc.3367

Alkyne hydrogenation using Pd–Ag hybrid nanocatalysts in surface-immobilized dendrimers

Edward A. Karakhanov[a]*, Anton L. Maximov[a,b], Anna V. Zolotukhina[a], Nadezhda Yatmanova[a] and Edward Rosenberg[c]*

A series of Pd–Ag mixed-metal nanocatalysts were prepared by reduction of Pd–Ag salts in the presence of poly(propylene imine) dendrimers, which were covalently bound to the surface of a silica polyamine composite, BP-1 (polyallylamine covalently bound to a silanized amorphous silica gel). Three different Pd-to-Ag ratios were evaluated (50:50, catalyst 1; 40:60, catalyst 2; 60:40, catalyst 3) with the goal of determining how the amount of Ag effects selectivity, rate and conversion in the selective reduction of alkynes, such as phenylacetylene and 1- or 4-octyne, to the corresponding alkenes. Conditions for the catalysis are reported where there is improved selectivity without a serious reduction in rate when compared with the analogous Pd-only catalysts. Catalyst 2 worked best for phenylacetylene and catalyst 3 worked best for the octynes. The catalysts could be reused seven times without loss of activity. Copyright © 2015 John Wiley & Sons, Ltd.

Additional supporting information may be found in the online version of this article at the publisher's web site.

Keywords: hydrogenation; palladium; silver; dendrimer; polyamine composite

Introduction

Catalytic hydrogenation is one of the most important processes in the modern petrochemical industry. Selective hydrogenation of the acetylenic and dienic fragments in C_2–C_5 hydrocarbons to their corresponding olefins avoids further polymerization and oxidation of these petroleum components.[1,2] The selective hydrogenation of phenylacetylene, which poisons polymerization catalysts, is more efficient than its separation from the feedstocks.[1,3,4]

The traditional heterogeneous catalysts used in industry frequently require vigorous reaction conditions and do not always have the ability to selectively reduce alkynes to alkenes, resulting in the necessity for additional separation processing. Homogeneous catalysts, which have high activity and selectivity, are not advantageous due to their high cost, low stability and the necessity to separate them from the reaction products for reuse.

Therefore, the synthesis of hybrid hydrogenation catalysts, which combine the merits of both homogeneous (high activity and selectivity) and heterogeneous (stability, recyclability) catalysts, is of current interest in the petrochemical industry. One approach to this type of system is the immobilization of metal complexes and/or metal nanoparticles in soluble polymers, bound to an inorganic carrier.[2,5–12]

Dendrimers, globular macromolecules with regular hyperbranched structures, are promising ligands for this goal.[13,14] Dendrimers possess the following advantages for use in catalysis:[13,15]

(1) good control over the quantity of metal sorption;
(2) provide a more even dispersion of particles on the carrier;
(3) better control of metal particle size, providing a material with a narrow size distribution;
(4) improved resistance to metal leaching; and
(5) allow the tuning of catalyst stability and substrate selectivity by means of dendrimer terminal group modification.

We have recently reported hydrogenations, catalyzed by Pd nanoparticles, which are stabilized by poly(propylene imine) (PPI) dendrimers immobilized on silica polyamine composites (SPCs).[16] This catalytic system proved very active for the selective hydrogenation of phenylacetylene to styrene and the reduction of dienes to monoenes. Very high turnover rates were realized and the catalyst could be reused multiple times without loss of activity.

The use of bimetallic nanoparticles in catalysis can offer higher selectivity and, sometimes, activity.[7,17–19] The addition of silver to a heterogeneous catalyst has been shown to be an effective additive for the semi-hydrogenation of phenylacetylene and other alkynes in the presence of palladium catalysts.[20,21]

In this paper we report the synthesis of catalysts based on palladium–silver nanoparticles, stabilized by PPI dendrimers, covalently grafted to a SPC in order to understand how the addition of silver would impact the selectivity and activity toward reduction of alkynes for this already efficient catalyst system. As in a previous study we used BP-1, a SPC based on polyallylamine (Fig. 1).

* *Correspondence to: Edward A. Karakhanov, Department of Petroleum Chemistry and Organic Catalysis, Moscow State University, 119991 Moscow, Russia. E-mail: kar@petrol.chem.msu.ru Edward Rosenberg, Department of Chemistry and Biochemistry, University of Montana, Missoula, MT 59812, USA. E-mail: edward.rosenberg@mso.umt.edu*

a *Department of Petroleum Chemistry and Organic Catalysis, Moscow State University, 119991 Moscow, Russia*

b *Institute of Petrochemical Synthesis RAS, 119991 Moscow, Russia*

c *Department of Chemistry and Biochemistry, University of Montana, Missoula MT 59812 USA*

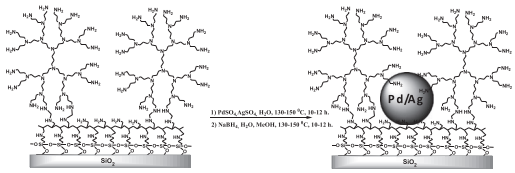

Figure 1. Synthesis of the bimetallic Pd–Ag catalyst.

Experimental

Materials

Reagents: phenylacetylene $C_6H_5C{\equiv}CH$ (98%, Aldrich); styrene $C_6H_5CH{=}CH_2$ (≥99%, Aldrich); ethylbenzene $C_6H_5CH_2CH_3$ (Reachim, Purum); 1-octyne (97%, Aldrich); 4-octyne (98%, Aldrich); 1-octene (Reachim, Purum); and *n*-octane (Reachim, Purum). Their purity was monitored by means of gas–liquid chromatography. Solvents methanol CH_3OH (>99%, Acros Organics), ethanol C_2H_5OH (Irea 2000, Purum p.a.) and *n*-hexane C_6H_{14} (Chimmed, Purum p.a.) were used without additional purification.

For the synthesis of the hybrid supports and catalysts the following substances were used: silver(I) sulfate Ag_2SO_4 (99%, Aldrich); palladium(II) sulfate $PdSO_4$ (98%, Aldrich); and sodium borohydride $NaBH_4$ (98%, Aldrich). PPI dendrimers of the third generation with a diaminobutane (DAB) core and 16 terminal amino groups (DAB $(NH_2)_{16}$) were synthesized according to a literature procedure.[22] The SPC material BP-1 was synthesized according to published literature procedures.[23,24]

Analyses

Chromatographic analysis of the reaction mixtures was done with a ChromPack CP9001 gas chromatograph equipped with a flame ionization detector and a 30 m × 0.2 mm column containing a grafted SE-30 phase. The chromatograms were recorded and analyzed with a computer using the Maestro 1.4 program. Conversion was determined from the change in the relative area (%) of substrate and product peaks.

Transmission electron microscopy (TEM) analysis was performed using a LEO912 AB Omega microscope with an electron tube voltage of 100 kV. The particle size distribution was measured by processing the obtained microscopy images using the ImageJ program. High-resolution TEM (HRTEM) analysis was performed using a JEM-2100 microscope with an electron tube voltage of 200 kV (LaB_6 cathode). The *d*-spacing of the metal nanoparticles was made by means of fast Fourier transforms of the micrographs obtained, using the ImageJ program.

X-ray photoelectron spectroscopy (XPS) studies were performed using a LAS-3000 instrument, equipped with a photoelectronic analyzer with retarding potential OPX-150. To excite photoelectrons, aluminum anode X-ray radiation was used (Al Kα = 1486.6 eV) with a tube voltage of 12 kV and emission current of 20 mA. The calibration of photoelectron peaks was performed along the C 1s line with binding energy of 285.0 eV. Deconvolution of palladium and silver peaks was processed with the PeakFit 4.11 program using the Gauss–Lorentz–Ampere approximation.

Quantitative determination of palladium and silver in the samples was performed using atomic emission spectroscopy with inductively coupled plasma (ICP-AES) using an IRIS Interpid II XPL instrument (Thermo Electron Corp., USA).

Synthesis of dendrimer-based hybrid materials

The synthesis of dendrimer-modified support $DAB(NH_2)_{16}$@BP-1 was carried out similar to a previously described procedure.[16] In a 10 ml single-neck round-bottom flask, equipped with a magnetic stirrer and a reflux condenser, 995 mg of the BP-1 support (1.6 mmol N g^{-1}, particle size range 250–550 μm), 300 μl of 37% aqueous formaldehyde solution (fivefold excess relative to the mmol N g^{-1} of BP-1) and 5 ml of methanol were combined. The reaction was carried out for 2 h with vigorous stirring, the product swelling to form a gel. The imine derivative of BP-1 formed was combined with the third-generation PPI dendrimer (600 mg, 0.356 mmol) and the reaction was conducted for 24 h at 70°C with vigorous stirring (the yellow-brown dendrimer solution gradually discolored). The mixture was evaporated using a rotary evaporator at 50°C. The product was isolated as a milky-white powder weighing 1.4 g (88% yield based on the dendrimer used).

XPS (eV): 102.2 (Si 2p, 6.0%); 285.2 (C 1s, 61.1%); 399.0 (N 1s, 16.0%); 531.2 (O 1s, 16.9%). ^{13}C NMR (δ, ppm): 71.0 ($HNCH_2OH$, $HNCH_2NH$); 53.5 (br s, $NCH_2CH_2CH_2N$, $(CH_2)_2CHCH_2NHCH_2$, $NCH_2CH_2CH_2CH_2N$); 41.6 (br s, $NCH_2CH_2CH_2NH_2$, $(CH_2)_2CHCH_2NH_2$); 28.0 (br s, $NCH_2CH_2CH_2NH_2$, $NCH_2CH_2CH_2N$); 18 (br s, $NCH_2CH_2CH_2Si$); 13 (br s, $NCH_2CH_2CH_2Si$). ^{29}Si NMR (δ, ppm): −65.2 (br, $Si(OSi)_3(CH_2)_3$); −97.0 (br, $Si(OSi)_3OH$); −111 (br s, $Si(OSi)_4$).

Catalyst ***1****: $DAB(NH_2)_{16}$*$Pd_{50}Ag_{50}$@BP-1*

In a single-neck round-bottom flask (capacity of 50 ml), equipped with a magnetic stirrer and a reflux condenser, 500 mg of the composite material $DAB(NH_2)_{16}$@BP-1 and 20 ml of water were placed. Then 95 mg (0.4675 mmol) of $PdSO_4$ and 73 mg (0.234 mmol) of Ag_2SO_4 (Pd:Ag mole ratio of 50:50) were added to the resulting suspension with stirring.

The reaction was carried out for 12 h at 80°C and with vigorous stirring. The color of the reaction mixture was brown. After reaction, the suspension was evaporated using a rotary evaporator at 60°C. The resulting material was a grey-brown powder weighing 667 mg (97% yield, based on the metal compounds used).

XPS (eV): 102.2 (Si 2p, 18.8%); 285.1 (C 1s, 45.9%); 336.2 (PdO_x $3d_{5/2}$, 0.5%); 337.1 (PdO $3d_{5/2}$, 0.3%); 338.3 (Pd^{2+} $3d_{5/2}$, 0.2%); 340.9 (PdO_x $3d_{3/2}$, 0.2%); 341.7 (PdO $3d_{3/2}$, 0.1%); 342.8 (Pd^{2+} $3d_{3/2}$, 0.1%); 366.8 ($Ag^IAg^{II}O_2$ $3d_{5/2}$, 0.7%); 368.3 (Ag^0 $3d_{5/2}$, 0.5%); 373.0 ($Ag^IAg^{II}O_2$ $3d_{3/2}$, 0.6%); 368.3 (Ag^0 $3d_{3/2}$, 0.3%); 398.6 (N 1s, 5.2%); 400.4 (Ag^+, PdO_x←N 1s, 5.1%); 402.8 (Pd^{2+}←N 1s, 4.1%); 531.4 (O 1s, 17.4%). ICP-AES (%): Pd, 4.16; Ag, 0.25.

Reduction of this precursor was performed using 300 mg suspended in 10 ml of methanol and 5 ml of deionized water in a single-neck round-bottom flask (capacity of 50 ml), equipped with a magnetic stirrer and a reflux condenser. Then 160 mg (9.935 mmol) of sodium borohydride and 5 ml of water were added portion-wise to the resulting suspension with stirring. The color of the reaction mixture turned black and vigorous gas evolution was observed. The reaction was carried out for 12 h at 80°C with stirring. After the reaction, the resulting solid mixture was washed with water and methanol to remove sodium borate salts, and the residue was isolated by centrifugation and dried. The resulting material was a black powder weighing 268 mg (97% yield, based on reduction of the metal in the precursor).

XPS: 102.9 (Si 2p, 26.1%); 285.1 (C 1s, 24.1%); 334.7 (Pd^0 $3d_{5/2}$, 0.5%); 336.1 (PdO_x $3d_{5/2}$, 0.4%); 337.8 (Pd^{2+} $3d_{5/2}$, 0.3%); 339.5 (Pd^0 $3d_{3/2}$, 0.4%); 340.5 (PdO_x $3d_{3/2}$, 0.3%); 342.4 (Pd^{2+} $3d_{3/2}$, 0.1%); 368.1 (Ag^0 $3d_{5/2}$, 0.6%); 369.8 ($Ag^IAg^{II}O_2$, sat $3d_{5/2}$, 0.5%);

371.2 (Ag_2O, sat $3d_{5/2}$, 0.3%); 373.9 (Ag^0 $3d_{3/2}$, 0.3%); 375.1 ($Ag^IAg^{II}O_2$, sat $3d_{3/2}$, 0.2%); 376.4 (Ag_2O, sat $3d_{3/2}$, 0.2%); 399.6 (N 1s, 4.8%); 401.1 (Ag^+, PdO_x←N 1s, 6.6%); 402.5 (Pd^{2+}←N 1s, 7.7%); 532.9 (O 1s, 26.6%). ICP-AES (%): Pd, 6.21; Ag, 0.49.

Catalyst ***2****: DAB$(NH_2)_{16}$*$Pd_{40}Ag_{60}$@BP-1*

The synthesis was carried out according to the procedures described above. Amounts of 200 mg of DAB$(NH_2)_{16}$@BP-1 support, 30 mg (0.1496 mmol) of $PdSO_4$ and 35 mg (0.1122 mmol) of Ag_2SO_4 were combined in 10 ml of deionized water providing a nominal Pd:Ag ratio of 40:60. The resulting catalyst precursor was grey-brown powder weighing 263 mg (99% yield based on the metal compounds used).

The reduction of this precursor was carried out using 263 mg with 142 mg (3.74 mmol) of sodium borohydride in a mixture of 5 ml of deionized water and 5 ml of methanol. The resulting species was a black powder weighing 202 mg (84% yield based on reduction of the metal in the precursor).

XPS (eV): 102.6 (Si 2p, 31.9%); 285.5 (C 1s, 45.9%); 367.6 (Ag_2O $3d_{5/2}$, 0.3%); 369.0 ($Ag^IAg^{II}O_2$, sat $3d_{5/2}$, 0.8%); 372.4 (Ag_2O $3d_{3/2}$, 0.2%); 373.9 ($Ag^IAg^{II}O_2$, sat $3d_{3/2}$, 0.4%); 398.0 (N 1s, 1.8%); 400.2 (Ag^+, PdO_x←N 1s, 4.6%); 402.2 (Pd^{2+}←N 1s, 1.9%); 532.8 (O 1s, 30.2%). ICP-AES (%): Pd, 4.34; Ag, 0.44.

Catalyst ***3****: DAB$(NH_2)_{16}$*$Pd_{60}Ag_{40}$@BP-1*

The synthesis was carried out according to the procedures described above. Amounts of 1000 mg of DAB$(NH_2)_{16}$@BP-1 support, 227 mg (1.122 mmol) of $PdSO_4$ and 117 mg (0.374 mmol) of Ag_2SO_4 in 25 ml of deionized water provided a nominal Pd:Ag ratio of 60:40. The resulting catalyst precursor was a black-brown powder weighing 1273 mg (95% yield based on the metal compounds used).

The reduction of this precursor was carried out using 1273 mg with 711 mg (18.7 mmol) of sodium borohydride in a mixture of 10 ml of deionized water and 15 ml of methanol. The resulting species was a black powder weighing 955 mg (74% yield based on reduction of the metal in the precursor).

XPS (eV): 103.2 (Si 2p, 2.8%); 285.1 (C 1s, 24.8%); 335.9 (PdO_x $3d_{5/2}$, 0.4%); 337.1 (PdO $3d_{5/2}$, 0.2%); 338.3 (Pd^{2+} $3d_{5/2}$, 0.1%); 340.5 (PdO_x $3d_{3/2}$, 0.4%); 341.7 (PdO $3d_{3/2}$, 0.2%); 342.9 (Pd^{2+} $3d_{3/2}$, 0.1%); 367.1 ($Ag^IAg^{II}O_2$ $3d_{5/2}$, 0.6%); 368.4 (Ag^I/Ag_2O_2 $3d_{5/2}$, 0.3%); 369.6 ($Ag^IAg^{II}O_2$, sat $3d_{5/2}$, 0.2%); 372.9 ($Ag^IAg^{II}O_2$ $3d_{3/2}$, 0.4%); 374.1 (Ag^I/Ag_2O_2 $3d_{3/2}$, 0.3%); 375.8 ($Ag^IAg^{II}O_2$, sat $3d_{5/2}$, 0.2%); 399.6 (N 1s, 7.5%); 401.4 (Ag^+, PdO_x←N 1s, 4.6%); 402.8 (Pd^{2+}←N 1s, 2.7%); 532.7 (O 1s, 35.3%). ICP-AES (%): Pd, 6.96; Ag, 0.22.

Protocol for catalytic experiments

The desired amounts of catalyst and substrate were placed into a thermostatically controlled steel autoclave, equipped with a glass test-tube insert and a magnetic stirrer. The autoclave was sealed, pressurized with hydrogen up 1 or 3 MPa and connected to the thermostat. The reaction was carried out at 80°C for 1 h or 15 min. The reactor was then cooled below room temperature and depressurized. The reaction products were analyzed using gas–liquid chromatography.

Reuse of catalyst **3** was carried out by hydrogenation of 1-octyne. For this purpose, 1 mg of catalyst **3** and 250 μl of 1-octyne were placed in a thermostatically controlled stainless steel autoclave, equipped with a glass test tube-insert and a magnetic stirrer. The autoclave was sealed, pressurized with hydrogen up to 1 MPa and connected to the thermostat. The reaction was conducted at 80°C for 15 min. Then, the reactor was cooled below room temperature and depressurized. The reaction products were separated by decantation and analyzed using gas–liquid chromatography. The catalyst located *in vitro* was used without additional loading, drying or purification in subsequent reaction cycles.

The turnover frequency in each catalytic reaction is reported as specific activity (SA) and was calculated as the ratio of the reacted substrate to the metal loading, expressed in moles per unit time:

$$SA = \frac{\text{Conversion} \times v_{\text{substr}}}{v_{\text{Pd}} \times t} \quad (1)$$

Results and discussion

Synthesis and characterization of hybrid catalysts

Immobilization of the dendrimers on the SPC BP-1 surface was carried out using the Mannich reaction, with formaldehyde as the linking agent.[16] The latter was added in fivefold excess relative to the available amino groups on BP-1 based on N analysis. The dendrimer was added to the reaction mixture 2 h later to minimize crosslinking between the dendrimer molecules.

The composition and structure of the synthesized hybrid materials were elucidated by means of XPS, TEM and solid-state ^{13}C NMR and ^{29}Si NMR spectroscopy.

The XPS spectrum of the modified support shows the presence of $(CH_2)_3N$ fragments, which are typical for dendritic and polyallylamine moieties, and the presence of Si–O and Si–C bonds.[25,26] In comparison with the original BP-1 material[23,24] there is a decrease in surface oxygen and silicon content by a factor of two (6.0 and 16.9%, respectively, versus 14.7 and 34.6%), while the atomic concentrations of carbon and nitrogen increase by approximately 50% (61.1 and 16.0%, respectively, versus 40.2 and 10.5%), indicating the dendrimers are successfully bound to the BP-1 surface.

The ^{13}C NMR spectrum of the dendrimer-modified DAB$(NH_2)_{16}$@BP-1 carrier (Fig. S1) contains the following signals: 13–20 ppm, corresponding to the alkyl chains that are directly bound to silicon; 28 ppm, corresponding to the β-CH_2 groups in the polyalkylamine fragments; 41.6 ppm, typical for α-CH_2 groups at primary amino groups both in dendrimers and in polyalkylamine fragments of the original BP-1 support; 53.5 ppm, assigned to the α-CH_2 groups at secondary and tertiary amino groups of the polyalkylamine fragments.[27–29] The signals at 71 ppm can be assigned to the methylene groups of the polymer attached to the N=CH_2, groups fragments, which are formed due to the interaction of formaldehyde with the surface amino groups of the BP-1 carrier.

TEM revealed areas with two different types of structure in DAB$(NH_2)_{16}$@BP-1. The first type is homogeneous and contains cells and channels of 3 nm in diameter, which are characteristic of microporous materials (Fig. S2). This corresponds to the silica. The second type of structure consists of dark sphere-like formations of 15–20 nm in diameter. This corresponds to the dendrimer-modified areas of the BP-1 carrier. The small spherical 'particles' of 1.5–1.7 nm in diameter can be assigned to the dendrimers themselves.

To investigate the effect of the addition of silver on the activity and selectivity of the synthesized hybrid catalysts, we prepared samples with nominal Pd:Ag ratios of 50:50 (**1**), 40:60 (**2**) and 60:40 (**3**). The synthesis of the bimetallic Pd–Ag nanoparticles was carried out using the co-complexation method, with aqueous solutions of $PdSO_4$ and Ag_2SO_4 followed by reduction with $NaBH_4$ (Fig. 1).[30]

All the materials obtained were characterized using ICP-AES, XPS and TEM. For the catalyst with Pd-to-Ag ratio of 50:50, the unreduced precursor was also characterized. Physicochemical

characteristics of the catalysts synthesized are summarized in the Tables 1 and S1.

According to deconvolution of the XPS data (Table 1; Fig. 2), silver prevails on the surface of all samples. The surface palladium content in catalyst **2** is apparently below the instrument detection limit, i.e. below 0.5%. Therefore, in spite of the co-complexation method used, we obtained so-called 'core–shell' catalysts, in which one of the metals (palladium) is predominantly located in the core of each particle, and the other metal (silver) is located on its surface, in agreement with previous reports.[21]

In the unreduced catalyst, both palladium and silver are present in both zero-valent and oxidized states (Table S2; Fig. S3). The presence of zero-valent palladium in the spectrum of the unreduced catalyst can be explained in terms of electron transfer from the dendritic amino groups to the bimetallic palladium–silver clusters, resulting in enamine formation.[31]

It should be noted that the interpretation of the silver spectra is complicated due to overlapping of the binding energy signals that are typical of each of three common valence states of silver: Ag^0 (367.9–368.4 eV), Ag_2O (367.6–368.5 eV) and $Ag^{I}Ag^{III}O_2$ (367.3–368.1 eV).[32–35] The silver oxide signals are negatively shifted due to decreasing binding energy relative to the Ag^0 state.[36,37]

Reduction with sodium borohydride results in an increase of the zero-valent forms of silver and, especially, palladium. Thus, the $Pd^0/(PdO + Pd^{2+})$ ratio in catalyst **1** is approximately 3, whereas in the unreduced precursor this ratio does not exceed 1 (Table S1).

The prevalence of the oxidized forms of palladium in catalyst **3** (Table S1) can be explained in terms of the sample's facile oxidation on storage under ambient conditions.[38] The predominance of surface silver oxides in catalysts **2** and **3** (Table S2) can be explained in the same way. All the silver in catalyst **2** is apparently located on the nanoparticle surfaces, and results in its occurrence only as oxides (Table S1). This explains the absence of palladium in the spectrum of catalyst **2**.

TEM reveals that both large particles of 5–15 nm in diameter and small particles of 2–4 nm in diameter are present in the sample of the unreduced catalyst (Fig. 3(a)), but the smaller particles predominate, accounting for up to 99% of the total particles. Reduction by sodium borohydride of catalyst **1** results in a slight decrease in the number of small particles (down to 96%) and a shift of the large particles to a maximum of 4–6 nm (Fig. 3(b)). On the evidence of the data presented, we suggest that small particles are formed predominantly inside the dendrimer branches, while large particles grow in the areas with low grafted dendrimer density.

Changing the Pd-to-Ag ratio does not affect the mean diameter and distribution curve of the particles (Figs. 3(c) and (d)). However, increasing the silver content in catalyst **2** increases the average diameter of the larger particles to 4–8 nm (Fig. 3(c)).

Catalyst **3**, with a nominal Pd-to-Ag ratio of 60:40, was also characterized by means of HRTEM, which reveals both large (6–10 nm in diameter) and small (2–4 nm in diameter) particles (Fig. 4). According to the fast Fourier transform data, obtained after micrograph processing, the sample contains palladium, silver and palladium–silver nanoparticles, where the silver is dominant and both metals are predominantly in the oxidized states, in agreement with the XPS data.

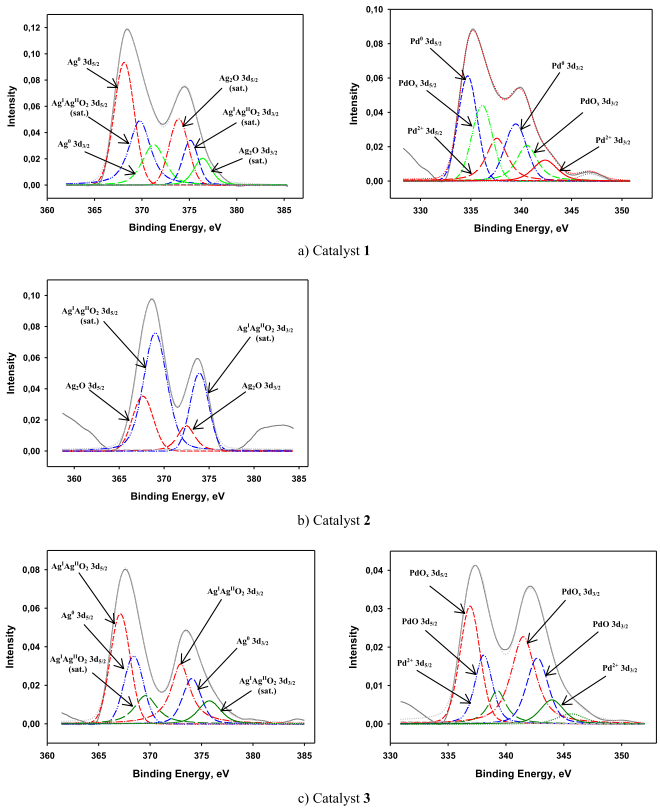

Figure 2. Deconvoluted XPS spectra: (a) catalyst **1** (50:50 Pd/Ag); (b) catalyst **2** (40:60 Pd/Ag); (c) catalyst **3** (60:40 Pd/Ag). The 3d silver spectra are left and the 3d palladium spectra are right.

Hydrogenation of unsaturated compounds in the presence of hybrid bimetallic catalysts

Phenylacetylene hydrogenation

The activity of the catalysts synthesized was investigated for phenylacetylene hydrogenation and calculated in terms of the ratio of the substrate reacted to the metal loading, expressed in moles per unit time, according to equation (1).

The results for catalyst **1** (Table 2) show that the presence of silver significantly increases the selectivity for styrene, while reducing activity in comparison with analogous palladium-only hybrid catalysts.[16] Thus, the selectivity for styrene is 97% at 15 min and a substrate-to-Pd ratio of 7780, but the conversion is only 40% (Table 2, entry 3). This indicates that the decreased activity of the

Table 1. Physicochemical characteristics of synthesized catalysts

SSample	Catalyst	Pd (mass %)	Ag (mass %)	*d* (nm)	XPS (at.%)					
					Si	C	N	O	Pd	Ag
Not reduced	$DAB(NH_2)_{16}$*$Pd_{50}Ag_{50}$@BP-1	4.16	0.25	2.5 (99%); 10.8 (1%)	18.8	45.9	14.4	17.4	1.4	2.1
1	$DAB(NH_2)_{16}$*$Pd_{50}Ag_{50}$@BP-1	6.21	0.49	2.5 (96.5%); 5.1 (3.5%)	26.1	24.1	19.1	26.6	2.0	2.1
2	$DAB(NH_2)_{16}$*$Pd_{40}Ag_{60}$@BP-1	4.34	0.44	2.4 (96%); 6.9 (4%)	31.9	27.9	8.3	30.2	-	1.7
3	$DAB(NH_2)_{16}$*$Pd_{60}Ag_{40}$@BP-1	6.96	0.22	2.5 (99.5%); 9.2 (0.5%)	2.8	24.8	14.8	35.3	1.4	2.0

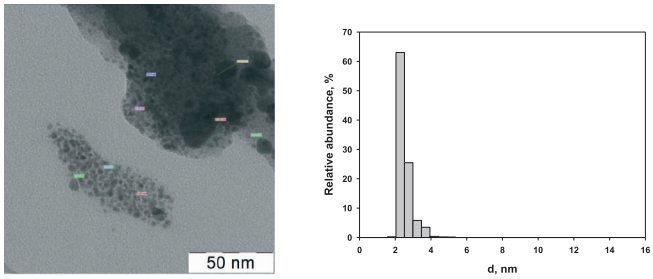

a) unreduced catalyst with Pd : Ag = 50 : 50

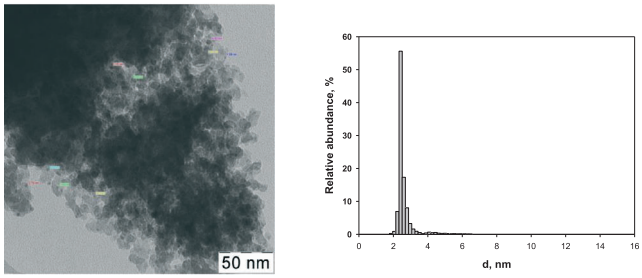

b) reduced catalyst with Pd : Ag = 50 : 50

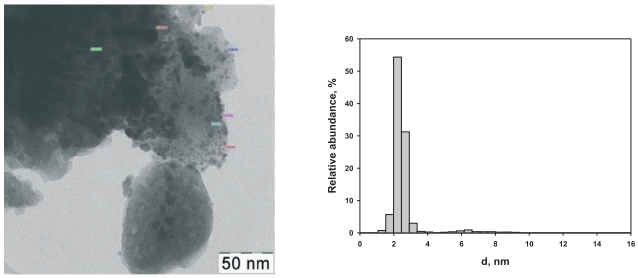

c) reduced catalyst with Pd : Ag = 40 : 60

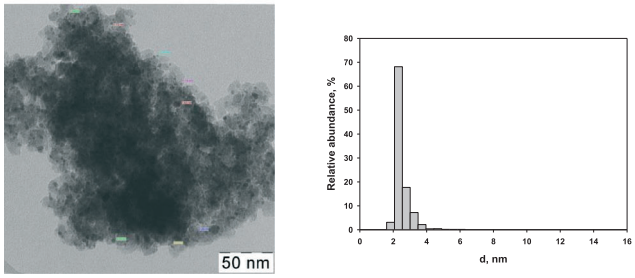

d) reduced catalyst with Pd : Ag = 60 : 40

Figure 3. TEM images and particle size distributions of the synthesized hybrid Pd–Ag catalysts.

synthesized Pd–Ag catalyst is due to the location of the catalytically active palladium atoms predominantly in the core of the particles, while the inactive silver atoms dominate on the surface.[20,21] Increasing the hydrogen pressure to 3 MPa results in an increase of the conversion (from 40 to 98%) while only slightly decreasing the selectivity (from 98 to 91%; Table 2, entry 4). We consider these reaction conditions to be the best for phenylacetylene semi-hydrogenation using catalyst **1**. Further increases in the substrate-to-Pd ratio lead to a decrease in conversion and increase in selectivity again. When starting with the unreduced precursor of **1**, the resulting catalyst is significantly less active, but more selective, than reduced catalyst **2** (Table S2).

Catalyst **2** does not contain Pd on its surface, as the XPS data reveal, and this is manifested in its much lower activity for phenylacetylene hydrogenation. Thus, at a substrate-to-Pd ratio of

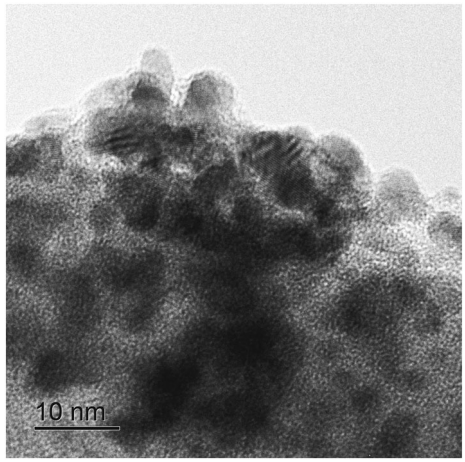

Figure 4. HRTEM image of catalyst **3**.

Table 2. Phenylacetylene hydrogenation (at 80°C) in the presence of catalyst **1**

Entry	*t* (min)	*P* (MPa)	Substrate/Pd (mol/mol)	Conversion (%)	SA (h^{-1})[a]	Selectivity to styrene (%)
1	60	1	3 890	100	3 890	71
2	15	1	3 890	100	15 560	86
3	15	1	7 780	40	12 450	97
4	15	3	7 780	98	30 505	91
5	15	3	15 565	42	26 145	98

[a]Specific activity calculated from equation (1).

5565 the conversion is close to quantitative after 90 min with a selectivity of 96% (Table 3, entry 2). Further decreasing the reaction time and increasing the substrate-to-Pd ratio lead to predictable decreases in the reaction yield, but the selectivity is still 96–98%.

Catalyst **3** appears to be more active than catalyst **2**, but less active than catalyst **1**. Also, it is significantly less selective than all the other catalysts (Table 4). We suggest that this behavior can be explained in terms of both the lower surface palladium content in comparison with silver and the palladium oxidized states being predominant. The latter results in a change in the adsorption properties of the catalyst; that is, the electron-deficient palladium oxide areas of the catalyst nanoparticles will more easily adsorb styrene as it is formed than areas containing palladium in reduced states (catalyst **1**) or of lower palladium content (catalyst **2**).

Table 3. Phenylacetylene hydrogenation (at 80°C) in the presence of catalyst **2**

Entry	*t* (min)	*P* (MPa)	Substrate/Pd (mol/mol)	Conversion (%)	SA (h^{-1})[a]	Selectivity to styrene (%)
1	120	1	5 565	100	2 780	75
2	90	1	5 565	97	3 600	96
3	60	1	5 565	83	4 620	97
4	15	1	5 565	34	7 570	97
5	15	1	11 135	17	7 570	98
6	60	3	11 135	35	15 590	96

[a]Specific activity calculated from equation (1).

Table 4. Phenylacetylene hydrogenation (at 80°C) in the presence of catalyst **3**

Entry	*t* (min)	*P* (MPa)	Substrate/Pd (mol/mol)	Conversion (%)	SA (h^{-1})[a]	Selectivity to styrene (%)
1	60	1	3470	99	3 435	50
2	15	1	3470	89	12 360	90
3	15	1	6940	40	11 110	91
4	15	1	6940	77	21 385	92

[a]Specific activity calculated from equation (1).

It should be noted that catalyst **3** appears to be much more resistant to air oxidation on storage. Therefore, it was used in further experiments for the hydrogenation of 1-octyne and 4-octyne.

Octyne hydrogenation

The hydrogenation of 1-octyne proceeds with the formation of 1-octene, octane and isomeric octenes, the latter being formed by palladium-catalyzed proton migration along the carbon chain (Scheme 1). Also, due to the sterically hindered dendritic matrix, grafted to the SPC surface, octane formation is possible only from 1-octene with its terminal double bond.

Conversion of 1-octyne to mainly 1-octene (68%) is observed at a reaction time of 15 min and a substrate-to-Pd ratio of 3470 (Table 5, entry 2). Increasing the reaction time to 60 min results in further hydrogenation of 1-octene to octane, whose yield reaches 60%, and an increased proportion of isomerized alkenes. Increasing the substrate-to-Pd ratio leads to a gradual decrease in conversion and a simultaneous increase in the selectivity for 1-octene. Thus, conversion to 1-octene is 31% and selectivity is 93% (SA = 17 220 h^{-1}) for 15 min at substrate-to-Pd ratio of 13 885. Increasing the reaction time to 60 min at this substrate-to-Pd ratio yields 100% conversion, but the proportion of 1-octene among the reaction products decreases to 52%. Conducting the experiment at the same substrate-to-Pd ratio with a hydrogen pressure of 3 MPa results in a conversion of 54% for 15 min, with the selectivity to 1-octene decreasing from 93 to 88% (Table 5, entry 6).

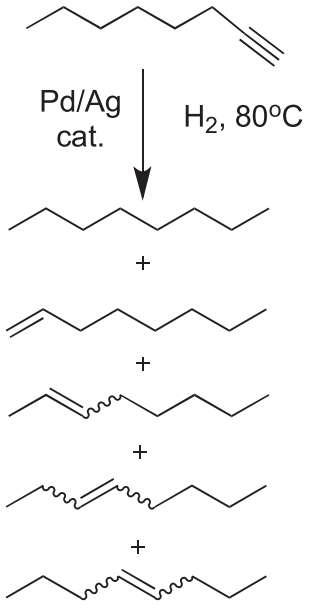

Scheme 1. Hydrogenation of 1-octyne in the presence of Pd-containing catalysts.

The optimal conditions for hydrogenation of 1-octyne to 1-octene with catalyst **3** are found to be a substrate-to-Pd ratio of 6940, a hydrogen pressure of 1 MPa and a reaction time of 15 min. This results in a conversion of 96% (SA = 26 660 h^{-1}), a total selectivity for alkenes of 86% and selectivity for 1-octene of 77% (Table 5, entry 3). These values for selectivity are slightly inferior to those obtained at a substrate-to-Pd ratio of 13 885 and a hydrogen pressure of 3 MPa (SA = 29 995 h^{-1}, total selectivity to alkenes of 91% and selectivity to 1-octene of 88%, but a lower conversion of only 54%).

The higher activity of catalyst **3** in the hydrogenation of 1-octyne as compared with phenylacetylene can probably be explained in terms of electron transfer from palladium to silver, as XPS results show (Table S2). On the other hand, dendrimer-based catalysts, containing only palladium, exhibit, as a rule, higher activity in the hydrogenation of conjugated double bonds.[16,39,40] We suggest this phenomenon can have two possible causes. The first one is that due to the silver prevailing on the surface of catalyst nanoparticles, there are left only a few sites favoring the plane-parallel adsorption of phenylacetylene and its subsequent hydrogenation. The second is that the C≡C triple bond in the molecule of phenylacetylene is more electron-deficient due to the weak −*M*-effect of the aromatic ring. In contrast, the alkyl substituent in the 1-octyne molecule provides a weak +*I*-effect. Therefore, its adsorption on the electron-deficient palladium surface is more favorable in comparison with phenylacetylene.

Hydrogenation of 4-octyne can proceed under both kinetic and thermodynamic control (Scheme 2; Fig. 5). Due to the facile isomerization of C=C bond in the presence of palladium catalysts, the sterically less hindered 2- and 3-octenes are formed at first as well as a small proportion of 1-octene. The order of their formation agrees with the remoteness of the newly formed C=C bond in the alkene from the C≡C triple bond in the initial 4-octyne. The higher concentration of the isomeric octenes is observed at a reaction time of 30 min, i.e. in the middle of the reaction process (Fig. 5). Subsequently, the reversal of isomerization takes place, and the thermodynamically more stable 4-octene is reformed. Hence, at a conversion of 100% for 60 min, the selectivity for 4-octene reaches 98%.

It should also be noted that due to the internal position of the C≡C bond in 4-octyne, its hydrogenation proceeds more slowly than that of 1-octyne. The specific activity for 4-octyne is 6940 h^{-1} at a substrate-to-Pd ratio of 3470. The further hydrogenation of 4-octyne at larger substrate-to-Pd ratios was not carried out, because the conversion for 15 min was only 49%.

Catalyst recycling

Recycling of catalyst **3** was carried out for the hydrogenation of 1-octyne. The protocol for the experimental procedure was similar to that for the standard hydrogenation procedure with the following difference. At the end of the each reaction cycle the products were separated by decantation, whereas the catalyst was kept in the glass test-tube and reused without additional loading and regeneration. Hexane was used as a solvent for the better resettling of the dendrimer-based catalysts.[6,41]

The results of the recycling test are shown in Fig. 6. The total turnover number for seven reaction cycles is 24 300. A slight coloring of the reaction mixture is observed after the first cycle, possibly indicating the formation of 1-octyne complexes with leached palladium in solution.[42–44] However, this decreases from cycle to cycle, and a decrease in the conversion is not observed suggesting

Table 5. Hydrogenation of 1-octyne (at 80°C) in the presence of catalyst **3**

Entry	*t* (min)	*P* (MPa)	Substrate/Pd (mol/mol)	Conversion (%)	SA (h^{-1})[a]	Products
1	60	1	3 470	100	3 470	1-Octene, 2%; 4-octene, 12%; other octenes, 26%; **octane, 60%**
2	15	1	3 470	100	13 885	**1-Octene, 68%**; 4-octene 6%; other octenes, 8%; octane, 18%
3	15	1	6 940	96	26 660	**1-Octene, 77%**; 4-octene, 3%; other octenes, 6%; octane, 14%
4	60	1	13 885	100	13 885	**1-Octene, 52%**; 4-octene, 7%; other octenes, 12%; octane, 29%
5	15	1	13 885	31	17 220	**1-Octene, 93%**; octane, 7%
6	15	3	13 885	54	29 995	**1-Octene, 88%**; 4-octene, 1%; other octenes, 2%; octane, 9%

[a]Specific activity calculated from equation (1).

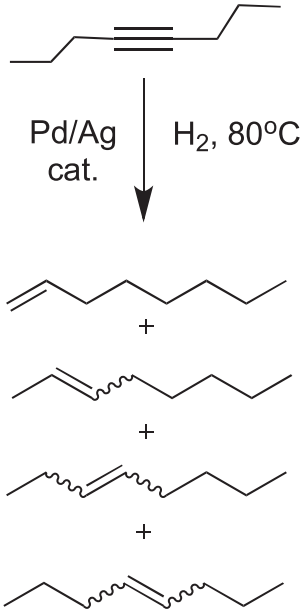

Scheme 2. Hydrogenation of 4-octyne in the presence of Pd-containing catalysts.

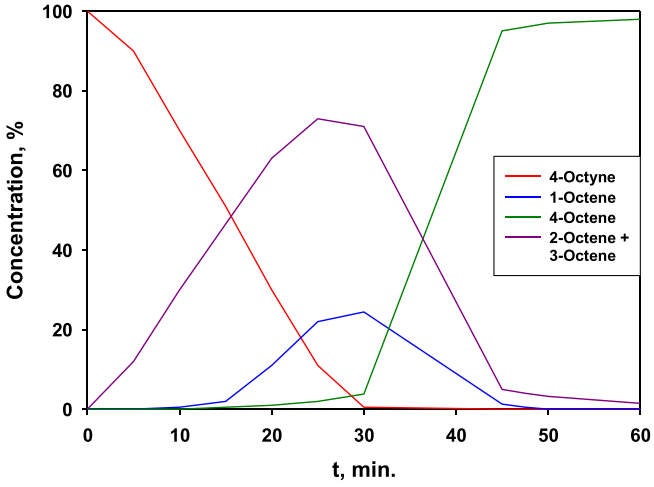

Figure 5. Kinetics of 4-octyne hydrogenation in the presence of catalyst **3**. (Reaction conditions: 80°C, 1 MPa of H_2, substrate/Pd ≈ 3470.)

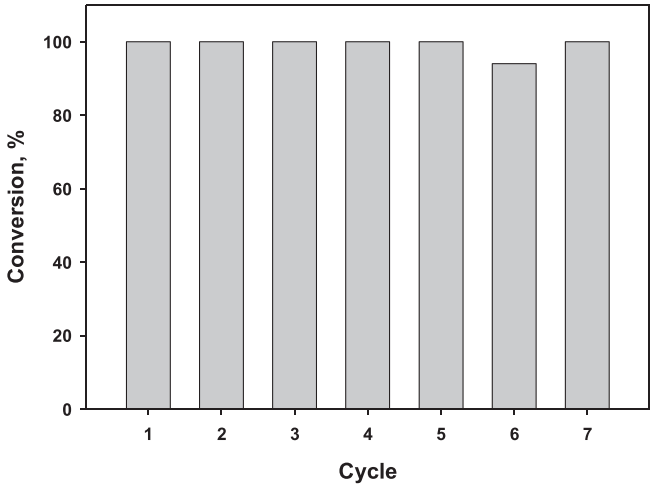

Figure 6. Recycling of catalyst **3** in the hydrogenation of 1-octyne. (Reaction conditions: 80°C, 1 MPa of H_2, 15 min, substrate/Pd ≈ 3470.)

that active metal leaching decreases after the first cycle.[45] Hence, the hybrid materials, based on the dendrimer-encapsulated Pd–Ag nanoparticles, can be reused without any loss of activity.

Conclusions

Two important conclusions can be drawn from this brief investigation. First, the XPS studies clearly demonstrate that the addition of silver to the hybrid palladium catalysts results in the formation of core–shell nanoparticles where silver dominates the outer shell. This leads to the second conclusion that the addition of silver mitigates catalyst activity and, as a result, improves selectivity for reduction of alkynes to alkenes due to the decreased palladium surface sites. However, by careful adjustment of hydrogenation conditions, good conversion of alkyne to alkene can be achieved with a reasonable selectivity. The arylalkyne phenylacetylene showed distinctly different behavior from that of 1-octyne and 4-octyne due to their different electronic properties (−*M* versus +*I*, respectively). Finally, the Pd–Ag hybrid catalyst can be reused without loss of activity.

Acknowledgements

This work was supported by RFBR grant no. 14-03-31531. We also acknowledge the National Science Foundation (CHE-1049569) for

support of this research. Also, we thank Natalia Tabachkova (National University of Science and Technology 'MISIS', Moscow, Russia) for HRTEM facilities.

References

[1] T.-B. Lin, T.-C. Chou, *Appl. Catal. A* **1994**, *108*, 7–19.
[2] J. Allen, E. Rosenberg, E. Karakhanov, S. V. Kardashev, A. Maximov, A. Zolotukhina, *Appl. Organomet. Chem.* **2011**, *25*, 245–254.
[3] S. Huh, R. Touroude, *J. Catal.* **1988**, *114*, 411–421.
[4] I. M. Zhvanetskii, F. D. Klebanova, E. A. Katsman, A. S. Berenblyum, *Kinet. Catal.* **1990**, *31*, 777–782.
[5] H. Brunner, P. Panstel, S. Wieland, in *Applied Homogeneous Catalysis with Organometallic Compounds*, (Eds.: B. Cornils, W. Hoffmann), Wiley-VCH, Weinheim, **2002**, pp. 646–663.
[6] R. W. J. Scott, O. M. Wilson, R. M. Crooks, *J. Phys. Chem. B* **2005**, *109*, 692–704.
[7] Y.-M. Chung, H.-K. Rhee, *Korean J. Chem. Eng.* **2004**, *21*, 81–97.
[8] R. Andrés, E. de Jesús, J. C. Flores, *New J. Chem.* **2007**, *31*, 1161–1191.
[9] J. M. Thomas, B. F. G. Johnson, R. Raja, G. Sankar, P. A. Midgley, *Acc. Chem. Res.* **2003**, *36*, 20–30.
[10] S. Boujday, J. Blanchard, R. Villanneau, J.-M. Krafft, C. Geantet, C. Louis, M. Breysse, A. Proust, *ChemPhysChem* **2007**, *8*, 2636–2642.
[11] J. Shen, X. Yin, D. Karpuzov, N. Semagina, *Catal. Sci. Technol.* **2013**, *3*, 208–221.
[12] S. Miao, Z. Liu, B. Han, J. Huang, Z. Sun, J. Zhang, T. Jiang, *Angew. Chem. Int. Ed.* **2006**, *45*, 266–269.
[13] Y. Niu, R. M. Crooks, *C. R. Chim.* **2003**, *6*, 1049–1059.
[14] G. R. Newkome, C. D. Shreiner, *Polymer* **2008**, *49*, 1–173.
[15] G. Jayamurugan, C. P. Umesh, N. Jayaraman, *J. Mol. Catal. A* **2009**, *307*, 142–148.
[16] E. Karakhanov, A. Maximov, Y. Kardasheva, V. Semernina, A. Zolotukhina, A. Ivanov, G. Abbott, E. Rosenberg, V. Vinokurov, *ACS Appl. Mater. Interfaces* **2014**, *6*, 8807–8816.
[17] A. R. Vilchis-Nestor, M. Avalos-Borja, S. A. Gómez, A. Hernández José, A. Olivas, T. A. Zepeda, *Appl. Catal., B* **2009**, *90*, 64–73.
[18] R. M. Crooks, M. Zhao, L. Sun, V. Chechik, L. K. Yeung, *Acc. Chem. Res.* **2001**, *34*, 181–190.
[19] H. K. Rhee, Y. M. Chung, *Catal. Lett.* **2003**, *85*, 159–164.
[20] G. C. Bond, A. F. Rawle, *J. Mol. Catal. A* **1996**, 109.
[21] N. A. Khan, A. Uhl, S. Shaikhutdinov, H. J. Freund, *Surf. Sci.* **2006**, *600*, 1849–1853.
[22] E. M. M. de Brabander-van den Berg, E. W. Meijer, *Angew. Chem. Int. Ed.* **1993**, *32*, 1308–1312.
[23] M. A. Hughes, D. Nielsen, E. Rosenberg, R. Gobetto, A. Viale, S. D. Burton, J. Ferel, *Ind. Eng. Chem. Res.* **2006**, *45*, 6538–6547.
[24] M. A. Hughes, E. Rosenberg, *Sep. Sci. Technol.* **2007**, *42*, 261–283.
[25] A. Tóth, I. Bertóti, V. S. Khotinsky, *Surf. Interface Anal.* **1994**, *22*, 551–555.
[26] P. Laoharojanaphand, T. J. Lin, J. O. Stoffer, *J. Appl. Polym. Sci.* **1990**, *40*, 369–384.
[27] G. R. Krishnan, K. Sreekumar, *Soft Matter* **2010**, *8*, 114–129.
[28] B. González, M. Colilla, C. López de Laorden, M. A. Vallet-Regí, *J. Mater. Chem.* **2009**, *19*, 9012–9024.
[29] A. Papp, K. Miklós, P. Forgo, Á. Molnár, *J. Mol. Catal. A* **2005**, *229*, 107–116.
[30] E. A. Karakhanov, A. L. Maximov, A. V. Zolotukhina, T. Y. Filippova, S. V. Kardashev, *Pet. Chem.* **2012**, *52*, 323–332.
[31] O. P. Parenago, V. M. Frolov, *Zh. Vses. Khim. O-va im. D. I. Mendeleeva* **1989**, *34*, 659–665(In Russian.).
[32] C. D. Wagner, A. V. Naumkin, A. Kraut-Vass, J. W. Allison, C. J. Powell, J. R. Rumble, NIST X-ray Photoelectron Spectroscopy Database, NIST Standard Reference Database 20, version 3.3, **2003**. Web version: http://www.srdata.nist.gov/xps/ (accessed April 2012).
[33] B. V. R. Chowdari, K. F. Mok, J. M. Xie, R. Gopalakrishnan, *J. Non-Cryst. Solids* **1993**, *160*, 73–81.
[34] P. Ptacek, Z. Bastl, *Appl. Surf. Sci.* **1990**, *45*, 319–323.
[35] V. K. Kaushik, *J. Electron Spectrosc. Relat. Phenom.* **1991**, *56*, 273–277.
[36] G. Schoen, *Acta Chem. Scand.* **1973**, *27*, 2623–2633.
[37] S. W. Gaarenstroom, N. Winograd, *J. Chem. Phys.* **1977**, *67*, 3500–3506.
[38] Z. Xiao, Y. Zhao, A. Wang, J. Perumal, D.-P. Kim, *Lab Chip* **2011**, *11*, 57–62.
[39] E. Karakhanov, A. Maximov, S. Kardashev, Y. Kardasheva, A. Zolotukhina, E. Rosenberg, J. Allen, *Macromol. Symp.* **2011**, *304*, 55–64.
[40] E. A. Karakhanov, A. L. Maximov, V. A. Skorkin, A. V. Zolotukhina, A. S. Smerdov, A. Y. Tereshchenko, *Pure Appl. Chem.* **2009**, *81*, 2013–2023.
[41] M. Murata, Y. Tanaka, M. Tomoo, K. Ebitani, K. Kaneda, *Chem. Lett.* **2005**, *34*, 272–273.
[42] M. Crespo-Quesada, R. R. Dykeman, G. Laurenczy, P. J. Dyson, L. Kiwi-Minsker, *J. Catal.* **2011**, *279*, 66–74.
[43] G. He, Y. Song, X. Kang, S. Chen, *Electrochim. Acta* **2013**, *94*, 98–103.
[44] M. Ahlquist, G. Fabrizi, S. Cacchi, P.-O. Norrby, *Chem. Commun.* **2005**, 4196–4198.
[45] W. Long, N. A. Brunelli, S. A. Didas, E. W. Ping, C. W. Jones, *ACS Catal.* **2013**, *3*, 1700–1708.

Supporting information

Additional supporting information may be found in the online version of this article at the publisher's web site.